Journal of the Serbian Chemical Society
JSCS-info@shd.org.rs • www.shd.org.rs/JSCS

ACCEPTED MANUSCRIPT

Journal of the Serbian Chemical Society
JSCS-info@shd.org.rs • www.shd.org.rs/JSCS
J. Serb. Chem. Soc. **00(0)** 1-17 (2026)
JSCS–13681
Original scientific paper
Published DD MM, 2026

Impact of silica gel G on mechanical and microstructural properties of magnesium oxychloride

NISHA YADAV[1], BHUPENDRA PAL[2], AND MEENAKSHI[1]*

[1]*Department of Chemistry, University of Rajasthan, Jaipur, Rajasthan,302004, India,*
[2]*Government Polytechnic College, Karauli, Rajasthan, 322241, India.*

(Received 17 December 2025; revised 19 January 2026; accepted 21 April 2026)

Abstract: Magnesium oxychloride cement (MOC), a type of Sorel's cement, has gained renewed attention as a sustainable building material due to its low carbon footprint and energy consumption. However, its application in construction remains limited, primarily due to its inadequate moisture resistance and the reduced early-age strength under elevated temperature conditions. This research investigates the impact of silica gel G (SG) on the properties of MOC. SG was incorporated into MOC at varying proportions (0-20% by weight of MgO) to form MOC-SG composites. The study evaluated the physical and mechanical properties of these composites, including setting time, moisture ingress resistance, and compressive strength. Additionally, FTIR, PXRD, SEM-EDX and TGA analysis were also conducted to examine the crystalline phase of the composites. SG acts as a binding agent, enhancing the strength and durability of the composite. This research demonstrates the potential of MOC-SG composite as a promising sustainable building material. Results indicate that the addition of 5% SG significantly improves the properties of MOC.

Keywords: cement; silica gel G; setting time; water resistance; compressive strength.

INTRODUCTION

Cement, a foundational material in human civilization and infrastructure development, has been utilized for centuries.[1] In recent years, there has been a growing interest in low-carbon cement alternatives, such as magnesium oxide-based cement. Magnesium oxychloride cement (MOC) was first developed in 1867 by S.T. Sorel.[2] In recent years, MOC, is gaining attention due to its low energy consumption and reduced CO_2 emissions.[3-7]

In comparison with ordinary Portland cement (OPC), MOC exhibits several noteworthy performance advantages, including high early and ultimate strength, strong interfacial bonding, rapid setting, low thermal conductivity, enhanced wear

* Corresponding author. E-mail: meenakshialwaraj@gmail.com
https://doi.org/10.2298/JSC251217021Y

resistance, favorable mechanical properties, dimensional stability, and excellent cohesiveness in lightweight composite panels.[8,9] Additionally, its inherent fire resistance and the absence of requirement for humid curing further contribute to its applicability across diverse construction contexts.[10]

MOC is frequently referred to as a green or eco-friendly cement due to its lower energy demand during synthesis with, requiring neither high-temperature processing nor external heat or light. The CO_2 emissions associated with MOC production are typically 40%–50% lower than OPC. Moreover, MOC continues to sequester CO_2 from the atmosphere after curing and does not release heat during curing, making it a viable and cost-effective substitute for energy-intensive OPC.

MOC is produced through the direct reaction between lightly calcined MgO and a concentrated $MgCl_2$ solution. This reaction is exothermic, and the heat generated can induce microcracking during the setting and curing stages. Such thermal microcracks facilitate water ingress, ultimately compromising the compressive strength and durability of the cement. To mitigate this issue, inert filler is incorporated into the MOC matrix. Acting through a collision-based heat absorption mechanism, this filler dissipates thermal energy without participating in the primary cementation reactions.[11] In the present study, dolomite powder was used as an inert filler to decrease thermal shock and minimize crack development in MOC (Eq. 1 and 2).

$$\mathrm{MgO\ (s) + MgCl_2{\cdot}6H_2O\ (liq.) \rightarrow MOC + Heat \rightarrow Cracking} \quad (1)$$

$$\mathrm{MgO\ (s) + MgCl_2{\cdot}6H_2O\ (liq.) + Inert\ filler \rightarrow MOC + Inert\ filler^{*}} \quad (2)$$

$$\downarrow$$

No cracking

Temperature, along with the molar ratios and relative concentrations of MgO, $MgCl_2$, and H_2O, plays a critical role in governing the hydration and mineral composition of MOC. These parameters strongly influence the formation, stability, and proportion of hydration products—typically represented as $xMg(OH)_2{\cdot}yMgCl_2{\cdot}zH_2O$—which in turn exert a direct effect on the resulting compressive strength of the material.[12,13]

Several distinct phase assemblages are known to form within the MgO–$MgCl_2$–H_2O system, including Phase-3 [$3Mg(OH)_2{\cdot}MgCl_2{\cdot}8H_2O$], Phase-5 [$5Mg(OH)_2{\cdot}MgCl_2{\cdot}8H_2O$], Phase-9 [$9Mg(OH)_2{\cdot}MgCl_2{\cdot}8H_2O$], and Phase-2 [$2Mg(OH)_2{\cdot}MgCl_2{\cdot}8H_2O$], typically stable across temperatures ranging from approximately 30 °C to 120 °C. The specific hydrate phases present in the hardened matrix are largely represented by the MgO/$MgCl_2$ molar ratio, which controls the reaction pathways and ultimate phase composition.

Under ambient conditions, Phase-5 and Phase-3 are the predominant and most thermodynamically stable hydration products in MOC systems, as represented in reactions (3) and (4).

$$5MgO + MgCl_2 + 13H_2O \rightarrow 5Mg(OH)_2 \cdot MgCl_2 \cdot 8H_2O \text{ (Phase-5)} \quad (3)$$

$$3MgO + MgCl_2 + 11H_2O \rightarrow 3Mg(OH)_2 \cdot MgCl_2 \cdot 8H_2O \text{ (Phase-3)} \quad (4)$$

These phases contribute significantly to the strength development, durability, and overall performance of MOC.

Although MOC exhibits a wide range of favorable mechanical and engineering properties, its large-scale industrial application remains significantly constrained. The primary limitations arise from its poor resistance to moisture and its susceptibility to reduced early-age strength when exposed to elevated temperatures. These drawbacks lead to excessive moisture uptake, dimensional instability, and structural deformability under humid or high-temperature conditions. Consequently, despite its promising performance attributes, the broader commercial adoption of MOC has been limited. Owing to its many advantageous characteristics, extensive research has been devoted to magnesium oxychloride cement, with numerous studies aiming to further enhance its performance and broaden its applicability. A wide range of inorganic, organic, and hybrid additives have been incorporated into MOC systems with the aim of enhancing properties such as moisture resistance, mechanical strength, dimensional stability, and overall durability.[14-25]

Numerous studies have demonstrated that incorporating silica-based materials such as silica fume, nano-silica, and others—either individually or in combination with supplementary additives like fly ash and phosphoric acid—significantly enhances the water resistance and overall performance of MOC. Silica fume, owing to its ultrafine particle size and high amorphous SiO_2 content, improves MOC mainly by micro-pores filling, microstructure densification, and promoting the formation of magnesium–silicate–hydrate or Mg–Cl–Si–H type gels, which have superior stability in moist environments compared with conventional MOC hydration phases.[26] Hybrid systems incorporating silica fume and fly ash often demonstrated synergistic effects, with improved long-term retention of strength after water immersion while maintaining adequate mechanical properties.[27,28] Nano-silica, owing to its high reactivity and surface area, further accelerates hydration, promotes secondary reactions of unreacted MgO, refines pore structure, and markedly reduces permeability. These effects translate into notable improvements in compressive strength and durability under wet conditions.[29] When nano-silica is combined with fly ash or phosphate-based modifiers, additional improvements arise owing to the formation and stabilization of water-resistant binding gels.[30] Collectively, the literature indicates that silica-based additives play a crucial role in mitigating the inherent water sensitivity of MOC by altering its hydration chemistry and microstructure.

Silica gel G (SG) is an amorphous form of SiO_2 containing approximately 13% gypsum, which contributes to its binding capability. This research study aims to introduce SG as a novel additive for MOC and evaluate its effect on the

material's physicochemical and mechanical properties. The investigation also examines dolomite as an inert filler alongside SG, considering its role in improving particle packing, dimensional stability, and resistance to shrinking-induced microcracking. The key objective is to determine whether the combined use of SG and dolomite can refine the MOC microstructure, lower capillary porosity, stabilize hydration products, and promote water-resistant binding phases, thereby improving durability and reducing the well-known susceptibility of MOC to strength loss under water exposure.

EXPERIMENTAL

Materials

In this study, magnesium oxide (MgO), magnesium chloride ($MgCl_2.6H_2O$), dolomite, and silica gel G (SG) were used as basic raw materials.

- Magnesium oxide (MgO): Lightly calcined commercial grade MgO was procured from Suksha Exports, Jaipur, Rajasthan, India. The chemical composition of MgO is: MgO = 89.90%, SiO_2 = 4.19%, CaO = 1.40%, Fe_2O_3 = 0.12%, and Al_2O_3 = 0.88%. The loss of ignition, brightness and whiteness of MgO is 3.08%, 88.20% and 91.60%, respectively.[31]
- Magnesium chloride ($MgCl_2.6H_2O$): Technical grade Magnesium chloride was procured from Alum Scientific Suppliers, Jaipur, Rajasthan, India. It is colourless crystalline and hygroscopic compound, which has 96.60% purity.[32]
- Dolomite: In this study, commercial grade dolomite was used as an inert filler and procured from Ases Chemical Works, Jodhpur, Rajasthan, India. The chemical composition of dolomite is: CaO = 28.00%, MgO = 18.00%, SiO_2 = 10.98%, Fe_2O_3 = 0.71%, and Al_2O_3 = 0.10%. The LOI, brightness and whiteness of dolomite is 41.80%, 89.40% and 92.70%, respectively.[33]
- Silica Gel G: In this study, SG was employed as a chemical admixture and procured from CDH Fine Chemicals, New Delhi, India.

Methods

The methods for the preparation of dry-mix composition, gauging solution and wet-mix composition with the incorporation of SG are given below:

- Preparation of dry-mix composition and incorporation of silica gel G: To prepare dry-mix, MgO and dolomite were gently mixed together in equal weight ratio. Powdered SG was also mixed in this dry-mix composition in varying weight proportions of 5%, 10%, 15% and 20% with respect to MgO. A control dry-mix was also prepared with no addition of SG.
- Preparation of gauging solution: To prepare gauging solution, sufficient amount of $MgCl_2.6H_2O$ powder was added to the lukewarm water (37°C) with continuous agitation till saturation point. This saturated solution of $MgCl_2$ is referred to as gauging solution for MOC. The concentration of saturated gauging solution was obtained approx. 31°Be on Baume Scale. Solution of $MgCl_2.6H_2O$ of 25°Be concentration was used as gauging solution in the present research work.
- Preparation of wet-mix: To form wet-mix, the gauging solution was blended into the dry-mix to get a workable wet-mix consistency. The incorporation of SG on the optimal cementing composition of MOC was investigated with this wet-mix composition. To obtain a uniform and workable paste, the solid-to-solution ratio was optimized

experimentally for each mix. For the compressive-strength specimens, the total solid mass (MgO + dolomite) was fixed at 540 g (MgO : Dolomite = 1:1) for compressive strength analysis (Table S1), and 200 g (MgO : Dolomite = 1:1) for setting time analysis, and the volume of $MgCl_2$ solution required for workable consistency varied with the SG content (Table S2).

In this study, each experimental procedure was repeated five times and the average was taken into account to get accurate readings. All experiments were performed under controlled environmental conditions, maintaining a constant temperature of 30°C and a relative humidity of approximately 90% throughout the testing period.

Investigation**:** Following procedures were conducted to investigate the effect of SG in MOC.

Setting time investigation

To find out the effect of SG on setting characteristics of MOC, different % (5%, 10%, 15%, & 20%) of SG were mixed with dry-mix composition (MgO: Dolomite = 1:1) in varying proportions. This mixture was then gauged with gauging solution to form a workable wet-mix. Standard procedure was adopted according to the Indian Standard (IS 10132-1982) specification to determine standard consistency. Vicat needle apparatus was used to calculate initial and final setting time.[33] Setting time blocks of simple MOC [M0 (only MgO and gauging solution)] and controlled MOC [M1 (MgO: dolomite = 1:1 with gauging solution)] were also prepared for comparative analysis. Results are reported in Figure 1.

Water ingress investigation

Moisture ingress tests were conducted on all previously prepared setting-time specimens to assess the effect of SG on the soundness of MOC. After a curing period of 60 days, the specimens (M0, M1, and various MOC–SG formulations) were subjected to boiling-water exposure, a procedure essential for evaluating their comparative moisture-sealing performance. A time-dependent assessment was then performed to determine the relative moisture resistance of each composition at successive intervals across a total duration of 30 hours. The measurements were recorded at the time intervals of 0–5, 5–10, 10–15, 15–20, 20–25, and 25–30 hours, to systematically monitor the progressive changes in the system. The comparative results of moisture-resistance performance for all specimen types are summarized in Table S3.

Compressive strength

To evaluate the influence of SG on the compressive strength of MOC, standard cube specimens of 70.6mm X 70.6mm X 70.6mm dimension with a surface area of 50 cm^2 were fabricated using various compositions [M0, M1, and MOC–SG formulations containing (5%, 10%, 15%, & 20% of SG)].[33] The dry mixtures were homogenized and subsequently gauged with the prepared gauging solution before being cast into molds. After remaining in the molds for 24 hours, the specimens were demolded and subjected to a 28-day curing period under controlled environmental conditions (temperature around 30 ^{0}C, and relative humidity above 90%). Compressive strength testing was performed using a universal testing machine in accordance with standard procedures (Figure S3). The results of the compressive strength measurements are presented in Figure 2.

Spectroscopic analysis

The effect of SG on the MOC block was also investigated through the following spectroscopic techniques on best modified MOC-SG composite.

- Fourier Transform-Infrared Spectroscopy (FT-IR): FT-IR spectra of MOC and SG incorporated MOC-SG composite cement were recorded using MRC-28 FT-IR analyzer in the range from 400 cm–1 to 4000 cm–1. For FT-IR spectra, the MOC cement samples were prepared in dehydrated potassium bromide.
- Powder X-Ray Diffraction (PXRD): PXRD diffraction pattern of MOC and SG incorporated MOC-SG composite cement were recorded using Panalytical X Pert Pro Diffractometer (Condition for diffraction pattern: 2θ = 5-70°, Cu Kα radiation, λ = 0.15406 Å).
- Microscopic analysis: Field Emission-Scanning Electron Microscopy (FE-SEM) images of MOC and SG incorporated MOC-SG composite were recorded using Jeol JSM- 7610F Plus FE-SEM Instrument. An EDS also performed for elemental analysis of MOC and MOC-SG composite samples.
- Thermogravimetric analysis: Thermogravimetric analysis (TGA) of MOC and SG incorporated MOC-SG composite cement was done using Perkin Elmer STA 6000 to find out the thermal stability. MOC and MOC-SG composite samples were heated under a nitrogen environment from room temperature to 800°C at a rate of 10°C per minute to obtain the results.

RESULTS AND DISCUSSION

Setting time analysis

Figure 1 illustrates the influence of varying SG concentrations (0-20%) on the initial and final setting times of the resulting composite. The exothermic reaction between MgO and $MgCl_2$ solution is responsible for the rapid setting of MOC. Hence the smallest initial and final setting time was observed for M0 without dolomite and additive.

In contrast, the control sample (M1) with half dolomite replacement exhibited relatively slower setting time than M0 due to the reduced exothermic reaction. Dolomite works as an inert filler, responsible for absorption of thermal shocks in situ in MOC by the three-body collision mechanism, as represented in reactions (1) and (2).

However, the addition of SG, a hydrophilic material, delays setting process. SG's strong hydrogen bonding capacity leads to increased water retention, hindering the hydration reaction and extending both the initial and final setting times. As the SG concentration rises, the water retention capacity increases, further delaying the setting process, and leading to a more controlled setting profile.

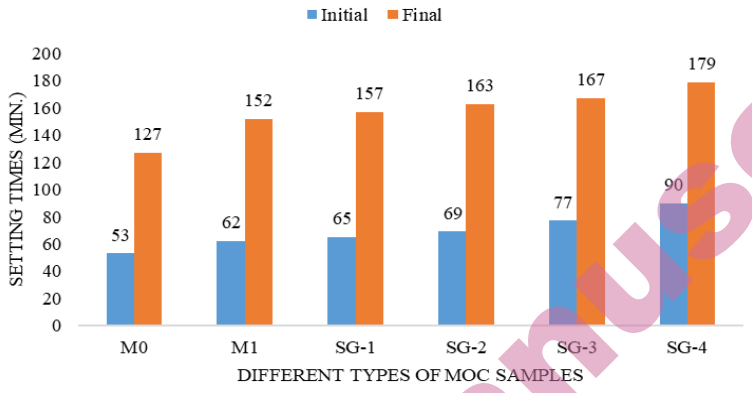

Fig 1. Setting times of M0, M1, and different types of MOC-SG samples.

Here:
M0 = MgO + gauging solution
M1 = (MgO : Dolomite = 1:1) + gauging solution
SG-1 = [(MgO : Dolomite = 1:1) + 5% SG] + gauging solution
SG-2 = [(MgO : Dolomite = 1:1) + 10 % SG] + gauging solution
SG-3= [(MgO : Dolomite = 1:1) + 15% SG] + gauging solution
SG-4 = [MgO : Dolomite = 1:1) + 20 % SG] + gauging solution

Analysis of water resistance

The water resistance characteristics of the MOC specimens are presented in Table S3. Owing to the highly exothermic reaction between magnesium oxide and the magnesium chloride solution, visible cracks developed in the M0 sample during the curing stage (Figure S1). During the subsequent water-resistance test, these cracks facilitated rapid water penetration, leading to their further widening and propagation. The increased permeability significantly accelerated water absorption and consequently diminished the overall water resistance of the M0 composition, rendering it unsuitable for structural applications.

In contrast, neither the M1 sample nor the SG-modified MOC specimens exhibited cracking during curing (Figure S2). The improved resistance to crack formation and water absorption can be attributed to the presence of dolomite, which effectively absorbs a portion of the heat generated during the exothermic reaction of the reactive components. By moderating the temperature rise, dolomite limits internal stress development and prevents crack initiation. The absence of cracks significantly restricts water ingress, thereby enhancing the overall durability of the cement matrix. Furthermore, dolomite contributes to improved water resistance by occupying internal voids and micro-pores within the hardened matrix. This pore-filling effect reduces the permeability of the cement, impeding water migration through the material and promoting the formation of a denser and more structurally sound matrix.

Compressive strength analysis: Figure 2 illustrates the compressive strength of MOC-SG composite blocks after a 28-day air curing period. The M0 sample, exhibited significant cracking during curing due to exothermic reaction between MgO & $MgCl_2$, rendering it unsuitable for construction applications (Figure S1). The sample M1, and different types of SG samples were free from cracks due to presence of dolomite (Figure S2). The addition of SG resulted in a notable enhancement in the compressive strength of the composite blocks. Specifically, the SG-1 sample demonstrated the highest compressive strength, surpassing both the control sample (M1) and samples with higher SG concentrations. The strong hydrogen bonding between the hydroxyl groups of SG and the MOC matrix likely contributed to the formation of inter-crossing crystals, leading to improved mechanical properties. However, excessive SG incorporation was found to be detrimental to the compressive strength. Therefore, the optimal SG concentration for enhancing the mechanical properties of MOC-SG composites was determined to be 5% by weight of MgO. Building upon the physical analysis results, M1 and SG-1 composite blocks were subjected to in-depth characterization using FT-IR and PXRD spectroscopic analysis.

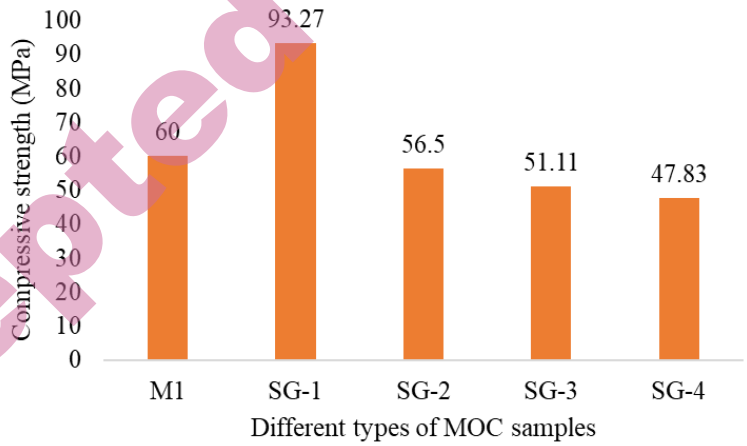

Fig 2. Effect of silica gel G on compressive strength characteristics of MOC-SG composite blocks.

FTIR analysis: FT-IR spectra of both M1 and SG-1 composite samples were recorded using KBr pellets in the range of 400-4000 cm^{-1} at ambient conditions. Figure 3 illustrates the FT-IR spectra of M1 and SG-1. Both M1 and SG-1 exhibited sharp, intense peaks in the 3600-3800 cm^{-1} region, characteristic of water molecule stretching vibrations.[34,35] However, the incorporation of SG resulted in broader, less intense peaks in this range, indicating a decrease in water content. This suggests that SG enhances the water resistance of the MOC-SG composite.

The stretching vibrations of crystalline hydroxyl groups were observed at 3695 cm^{-1} (M1) and 3698 cm^{-1} (SG-1), attributed to the stretching vibrations of the –OH group in brucite [$Mg(OH)_2$], suggest a low presence of $Mg(OH)_2$ in both samples. This is beneficial for the mechanical strength and moisture resistance of SG-1 composite sample.

The peaks at 1622 cm^{-1} (M1), 1611 cm^{-1} (SG-1), 3435 cm^{-1} (M1) and 3428 cm^{-1} (SG-1) originate from the crystalline phases, specifically Phase 5 [$5Mg(OH)_2 \cdot MgCl_2 \cdot 8H_2O$] and Phase 3 [$3Mg(OH)_2 \cdot MgCl_2 \cdot 8H_2O$], of the MOC matrix. The peak at 1385 cm^{-1} corresponds to the linear C-O bond vibration in carbonates. The peak at 1445 cm^{-1} (M1), & 1439cm^{-1} (SG-1) associated with C=O asymmetric stretching, becomes broader and more intense in SG-1, indicating interaction between the polar C=O group and the functional groups of SG. The out-of-plane bending of CO_3^{2-} is represented by peaks at 881 cm^{-1} (SG-1) and 880 cm^{-1} (M1)[3]. The absorption bands at 726 & 730 cm^{-1} (M1 and SG-1), 530 cm^{-1} (SG-1) and 542 cm^{-1} (M1), are attributed to the stretching and bending vibrations of Si-O, Mg-O, and Mg-Cl, respectively. Peaks at 1611cm^{-1} (SG-1) and 1622 cm^{-1} (M1) can be attributed to O-H bending vibrations. The presence of dolomite is also shown by the carbonate absorption peak at 2530 cm^{-1} (SG-1) and 2527 cm^{-1} (M1). The reduction in O-H peak intensity suggested the formation of hydrogen bonds between the hydroxyl groups of MOC phases and silica gel G. This hydrogen bonding, facilitated by SG, creates a protective coating that enhances the bonding strength of the MOC.

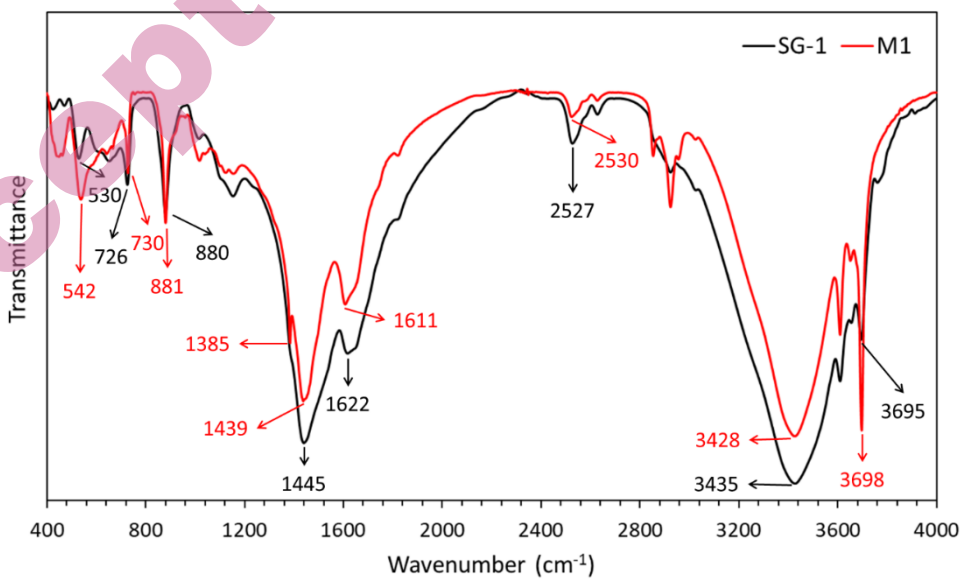

Fig 3. FT-IR spectra of M1 (Red) and Silica Gel G (SG) incorporated SG-1 (Black) composite samples.

Powdered XRD analysis: PXRD spectra of both M1 and SG-1 composite samples were recorded at ambient conditions and are presented in Figure 4. As evidenced by the diffraction patterns, the primary components of the MOC cement are Phase-5 [$5Mg(OH)_2 \cdot MgCl_2 \cdot 8H_2O$], unreacted MgO, brucite, and minor carbonated MgO. The characteristic reflections of MgO are indicated by peaks at $2\theta = 43°$ and 62.5°, indicating incomplete MgO hydration in both systems. The incorporation of 5% SG does not significantly introduce any new crystalline phases into the MOC composite matrix. The overall phase assemblage of SG-1 remains similar to that of M1, indicating that SG does not participate in crystallization as a distinct crystalline phase. However, a noticeable change in peak characteristics is observed. Compared to M1, the SG 1 pattern exhibits slightly reduced peak intensities accompanied by moderate peak broadening, which suggests a refinement of crystalline size and/or an increase in structural disorder. These changes are consistent with a modification of the hydration and crystallization process rather than a change in phase composition.

A particularly prominent peak at $2\theta = 31°$, associated with inert filler dolomite, is present in both samples with comparable intensity. This suggests that dolomite remains unreactive during hydration and functions as a heat-absorbing filler, without participating in the formation of hydration products. No distinct diffraction peaks attributable to SG are detected in SG-1. This observation is expected, as SG is predominantly amorphous in nature and therefore does not contribute sharp crystalline reflections in PXRD. The absence of additional peaks also confirms that SG does not form new crystalline reaction products with the MOC phases within the detection limits of PXRD. Instead, its presence is suggested to influence the nucleation and growth kinetics of Phase 5, which is also supported by the observed extension in setting time. The qualitative comparison of peak positions and relative intensities suggests that the incorporation of SG modifies the microstructural packing and crystallization behavior of the MOC matrix. This microstructural refinement is consistent with the experimentally observed improvements in water resistance and thermal stability of SG-1. The mechanical enhancement observed for SG-1 is therefore attributed to microstructural densification and improved phase interlocking, rather than an increase in the absolute amount of Phase 5.

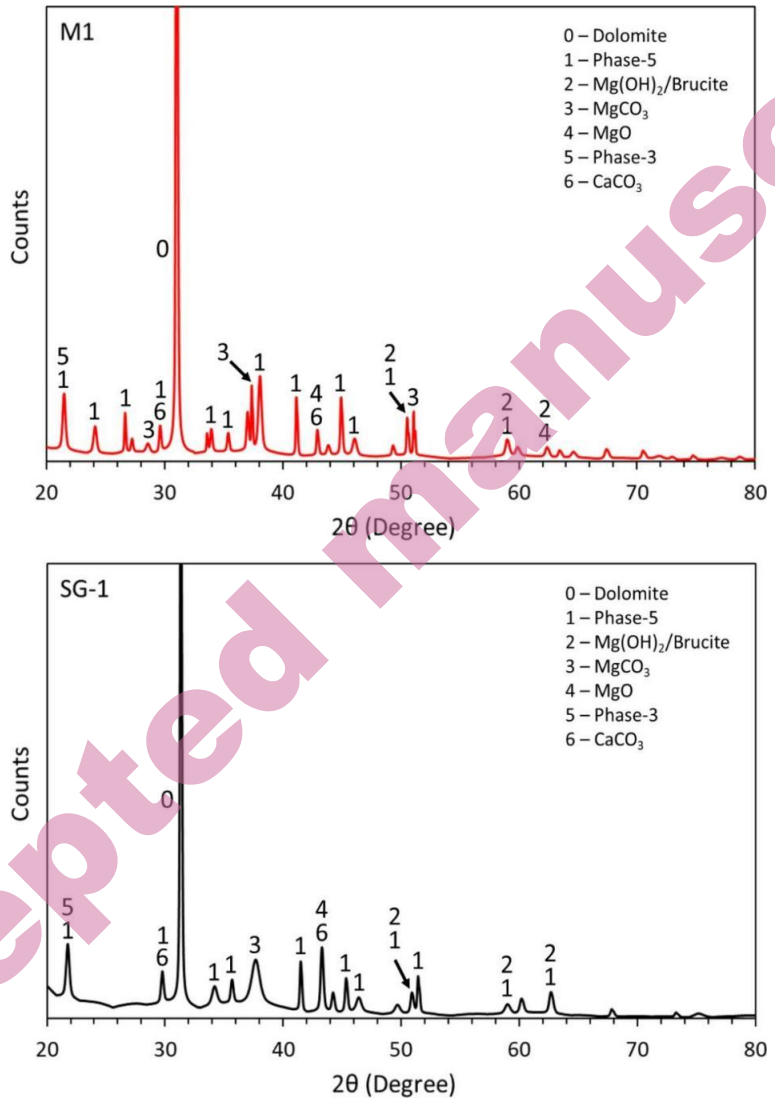

Fig 4. PXRD spectra of M1 and SG-1 samples.

SEM-EDX analysis: SEM-EDX analysis of both M1 and SG-1 were recorded and are shown in Fig. 5 and Fig. 6. The incorporation of silica gel G helped the rod-like phase- 5 crystals (M1) convert into gel-like amorphous phase-5 structure (SG-1), which could notably reinforce the mechanical property. It is also clear that the needle-like shape of the crystals was more clear in the SG-1 composite material than in M1. Due to needle-like crystals, the SG-1 has more interlocking Phase 5, which can be explained by the smaller void gap in SG-1 composite (Fig 8F) as compared to larger void gap in M1 (Fig. 8C). Therefore, SG-1 showed more

interlocking Phase-5 than M1, supporting enhanced strength and durability. In addition, the transformation of Phase-5 resulted in smaller voids in SG-1 so that the water resisting property of MOC was increased.

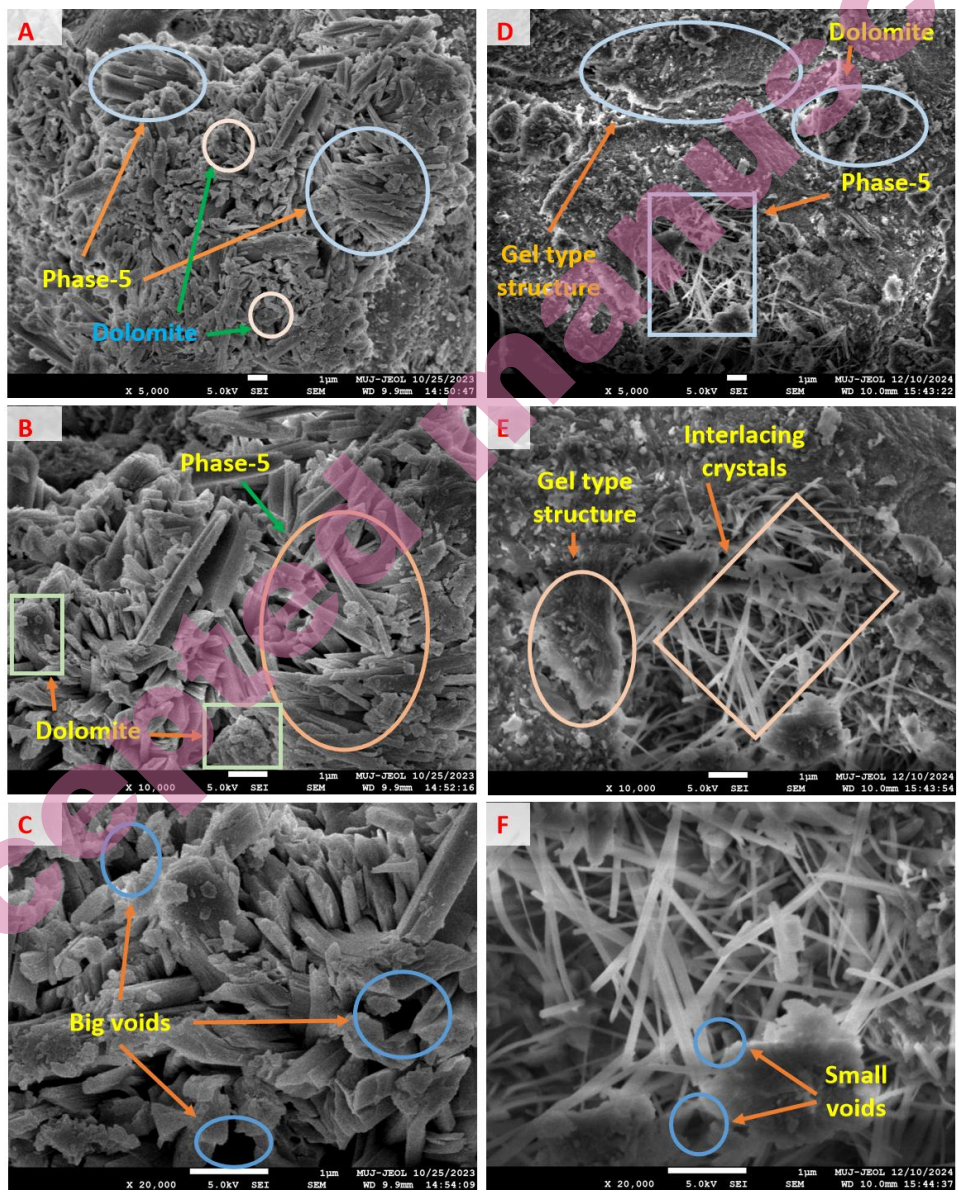

Fig 5. SEM images of M1 (A-C) and SG-1 (D-F) MOC-SG composite samples at different magnifications.

The SEM–EDX analysis (Figure 6) shows distinct differences in the elemental ratios of Mg, Cl, and O between M1 and SG-1. The molar ratio in M1 is 10.45 : 1.00 : 28.59, whereas SG-1 exhibits a ratio of 1.13 : 1.00 : 2.41. Rather than indicating the presence of amorphous phases, these differences reflect the relative proportions of magnesium-chloride–based hydration products formed in each mix. The higher Mg and Cl content in SG-1 suggests a greater formation of Phase 5–type MOC hydration products, consistent with the known role of silica additives in promoting Phase 5 development. This interpretation is in agreement with literature reports, which demonstrated that silica gel enhances both the quantity and crystalline size of Phase 5.[35] In contrast, the higher oxygen proportion in M1 is attributed to the larger amount of carbonate minerals present in the mix, rather than to any amorphous hydration product.

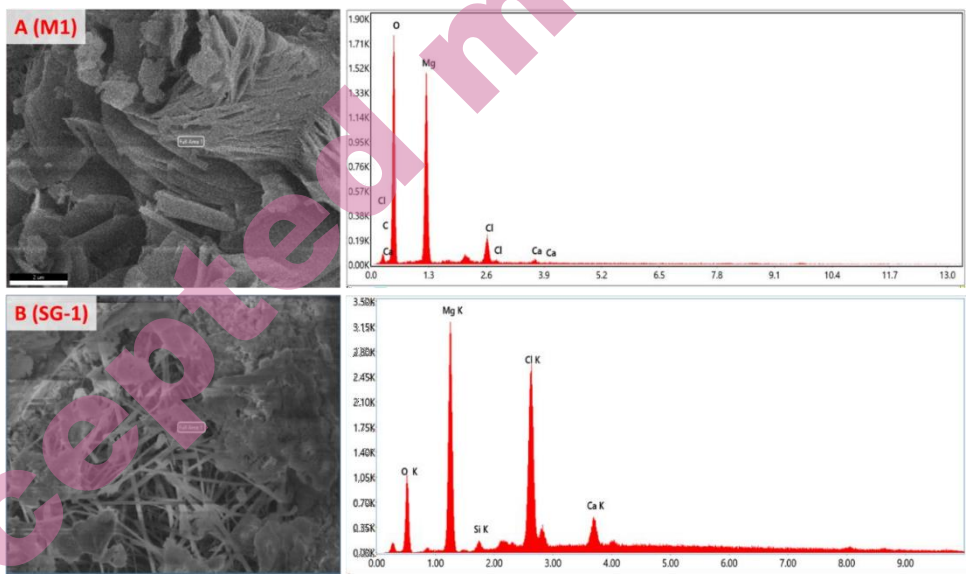

Fig 6. SEM-EDX of M1 (A) and SG-1 (B) MOC-SG composite sample.

Thermogravimetric analysis: The thermal decomposition of M1 and SG-1 can be seen from TGA curves in Figure 7. The decomposition takes place in three stages (Eq. 5 to 7). Both M1 and SG-1 sample mass loss are result of the slow evaporation of moisture (free water molecules), crystalline water, structural water, and hydrochloric acid (HCl) content throughout the heating process.[36,37] The weight loss in the first stage is nearly the same in both M1 and SG-1 samples, but slightly less weight loss was observed in SG-1. In the second stage, the weight loss increases in both M1 and SG-1 compared to the first stage weight loss and M1 has

more weight loss as compared to SG-1. In third stage, the weight loss decreases as compared to both first and second stages in M1. SG-1 has comparatively more weight loss in third stage as compared to M1. It was indicated that SG-1 is more thermally stable as lower temperature range (30°C to 430°C), but showed rapid decomposition at above 430°C to 730°C temperature range and become constant after 730°C. The overall weight loss in M1 and SG-1 is 44.80% and 38.04%, respectively, and therefore, SG-1 sample is thermally more stable as compared to M1.

$$5Mg(OH)_2 \cdot MgCl_2 \cdot 8H_2O \rightarrow 5Mg(OH)_2 \cdot MgCl_2 + 8H_2O \quad (5)$$

$$5Mg(OH)_2 \cdot MgCl_2 \rightarrow MgCl_2 \cdot H_2O + 5MgO \quad (6)$$

$$MgCl_2 \cdot H_2O \rightarrow MgO + 2\,HCl \quad (7)$$

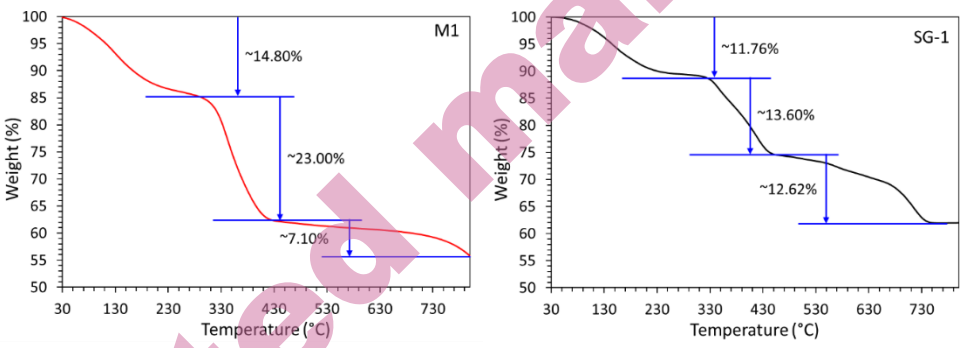

Fig 7. TGA of M1 and SG-1.

CONCLUSION

This research investigated the potential of silica gel G as an additive in magnesium oxychloride cement to enhance its properties and sustainability. The incorporation of SG in varying proportions (0-20% by weight of MgO) led to notable improvements in the physical and mechanical properties of the resulting MOC-SG composites. The mixing of SG into MOC significantly enhanced its physical and mechanical properties. Key findings includes:

Accelerated setting time: The addition of SG reduced the initial & final setting time of MOC, likely due to the decreased availability of MgO for the hydration reaction.

Enhanced mechanical strength: SG contributed to an increase in the compressive strength of MOC-SG composites, reaching an optimum value at around 5% SG content. This improvement is attributed to the formation of additional hydration products and the filling of pores by SG particles.

Improved thermal stability: The incorporation of SG enhanced the thermal stability of MOC-SG composites. This is likely due to the formation of a more stable crystalline structure and the reduced porosity of the composite.

Overall, the results of this study demonstrate the potential of silica gel G as a valuable additive for improving the performance of magnesium oxychloride cement. Further research is recommended to optimize the optimum dosage of silica gel G and explore its impact on other properties, such as durability and fire resistance.

SUPPLEMENTARY MATERIAL

Additional data are available electronically at the pages of journal website: https://www.shd-pub.org.rs/index.php/JSCS/article/view/13681, or from the corresponding author on request.

Acknowledgements: The authors are thankful to Department of Chemistry, University of Rajasthan, Jaipur, Rajasthan, India for providing over all support and the necessary laboratory facilities to fulfill the present research work. Financial support of this work has been provided by the CSIR-UGC, New Delhi, NTA Ref. No.: 201610163511.

И З В О Д

УТИЦАЈ СИЛИКА-ГЕЛА Г НА МЕХАНИЧКА И МИКРОСТРУКТУРНА СВОЈСТВА МАГНЕЗИЈУМ-ОКСИХЛОРИДА

NISHA YADAV[1], BHUPENDRA PAL[2] и MEENAKSHI[1]

[1]Department of Chemistry, University of Rajasthan, Jaipur, Rajasthan,302004, India, [2]Government Polytechnic College, Karauli, Rajasthan, 322241, India.

Магнезијум-оксихлоридни цемент (МОЦ), врста Сорел цемента, поново је добио на значају као одрживи грађевински материјал због малог угљеничног отиска и мале потрошње енергије. Међутим, примена овог цемента у грађевинарству остаје ограничена, првенствено због неадекватне отпорности на влагу и мале почетне чврстоће на повишеним температурама. У овом раду је испитиван утицај различитих количина силика гела Г (0-20 мас. % СГ) на својства добијених композита МОЦ-СГ. Анализирана су физичка и механичка својства ових композита, укључујући време везивања, отпорност на влагу и чврстоћу на притисак. Поред тога, спроведене су и FTIR, XRD, SEM-EDX и TGA анализе како би се испитале кристалне фазе композита и структурне карактеристике. SG делује као везивно средство, повећавајући чврстоћу и издржљивост композита. Ово истраживање показује потенцијал МОЦ-СГ композита као обећавајућег одрживог грађевинског материјала. Резултати показују да додавање 5% СГ значајно побољшава својства МОЦ-а.

(Примљено 17. децембра 2025; ревидирано 19. јануара 2026; прихваћено 21. априла 2026.)

REFERENCES

1. A. Bentur, *J. Mater. Civ. Eng.*, **14** (2002) 2 (https://doi.org/10.1061/(ASCE)0899-1561(2002)14:1(2))
2. S. T. Sorel, *Comptes Rendus hebdomadaires des Séances de l'Académie des Sciences, Paris, France* **65** (1867) 102 (https://gallica.bnf.fr/ark:/12148/bpt6k3022r/f104.item)
3. S. A. Walling, J. S. Provis, *Chem. Rev.* **116** (2016) 4170-4204 (https://doi.org/10.1021/acs.chemrev.5b00463)

4. D. Meng, C. Unluer, E. H. Yang, S. Qian, *Cem. Concr. Compos.* **138** (2023) 104983 (https://doi.org/10.1016/j.cemconcomp.2023.104983)
5. W. Shen, L. Cao, Q. Li, Z. Wen, J. Wang, Y. Liu, R. Dong, Y. Tan, R. Chen, *J. Clean. Prod.* **131** (2016) 20 (https://doi.org/10.1016/j.jclepro.2016.05.082)
6. L.Wang, L. Chen, D.C.W. Tsang, *Green remediation by using low-carbon cement-based stabilization/solidification approaches*, in *Sustainable Remediation of Contaminated Soil and Groundwater*, D. Hou, Ed., *Butterworth-Heinemann* (2020) pp. 93-118 (https://doi.org/10.1016/B978-0-12-817982-6.00005-7)
7. M. Costato, *Il Nuovo Cimento D* **17** (1995) 545 (https://doi.org/10.1007/BF02451742)
8. A. Maier, D. L. Manea, *Materials,* **15** (2008) 1772 (https://doi.org/10.3390/ma15051772)
9. Q. Huang, W. Zheng, J. Dong, J. Wen, C. Chang, X. Xiao, *J. Build. Eng.* **57** (2022) 104923 (https://doi.org/10.1016/j.jobe.2022.104923)
10. R. N. Yadav, P. Gupta, *Adv. Cem. Res.,* **26** (2014) 319. (http://dx.doi.org/10.1680/adcr.13.00036)
11. Meenakshi, *Asian J. Chem.* **35** (2023) 869 (https://doi.org/10.14233/ajchem.2023.26992)
12. N. Zhang, H. Yu, H. Ma, H. Ma, M. Ba, *Composites Part B Eng.* **247** (2022) 110328 (https://doi.org/10.1016/j.compositesb.2022.110328)
13. Y. Guan, Z. Hu, Z. Zhang, J. Chang, W. Bi, C. R. Cheeseman, T. Zhang, *Cem. Concr. Res.* **143** (2021) 106387 (https://doi.org/10.1016/j.cemconres.2021.106387)
14. R. A. S. Alatawi, N. H. Elsayed, W. S. Mohamed, *J. Mater. Res. Technol.* **8** (2019) 244 (https://doi.org/10.1016/j.jmrt.2018.01.010)
15. C. Guo, N. Chen, R. Wang, *J. Build. Eng.* **98** (2024) 111070 (https://doi.org/10.1016/j.jobe.2024.111070)
16. C. Li, N. Zhou, P. Guo, M. Li, F. Wang, J.Li, Y. Han, Z. Wu, W. Lu, *Adv. Compos. Hybrid Mater.* **8** (2025) 43 (https://doi.org/10.1007/s42114-024-01129-5)
17. Y. Li, Z. Li, H. Pei, H. Yu, *Constr. Build. Mater.* **102** (2016) 233 (https://doi.org/10.1016/j.conbuildmat.2015.10.186)
18. B. Şimşek, *Constr. Build. Mater.* **320** (2022) 126250. (https://doi.org/10.1016/j.conbuildmat.2021.126250)
19. Y. Yin, J. Huang, T. Wang, R. Yang, H. Hu, M. Manuka, F. Zhou, J. Min, H. Wan, D. Yuan, B. Ma, *Constr. Build. Mater.* **405** (2023) 133347 (https://doi.org/10.1016/j.conbuildmat.2023.133347)
20. Z. Qin, J. Wu, Z. Hei, L. Wang, D. Lei, K. Liu, Y. Li, *Materials* **17** (2024) 2053 (https://doi.org/10.3390/ma17092053)
21. L. Wang, Z. Qin, J. Wu, G. Sheng, H. Wang, K. Liu, X. Dong, F. Wang, J. Jiang, *Buildings* **14** (2024) 41 (https://doi.org/10.3390/buildings14010041)
22. M. Harun, U. Ali, M. Aziz, M. A. Mohamed, H. R. Khalid, S. Ahmad, A. Hanif, *Res. Eng.* **27** (2025) 105915 (https://doi.org/10.1016/j.rineng.2025.105915)
23. F. Ahmed, S. Rawat, Y. Zhang, *Appl. Sci.* **14** (2024) 3074 (https://doi.org/10.3390/app14073074)
24. H. M. Hamada, A. Al-Attar, M. K. Askar, S. Beddu, A. Majdi, *Int. J. Concr. Struct. Mater.* **19** (2025) 76 (https://doi.org/10.1186/s40069-025-00808-x)
25. H. Zhang, A. Luo, L. Sun, *Sci. Rep.* **14** (2024) 11656 (https://doi.org/10.1038/s41598-024-62602-1)
26. W. Chen, C. Wu, F. Chen, S. Zheng, Effects of silica fume on water-resistant property of magnesium oxychloride cement*, Advances in Engineering Research, Proceedings of the*

2017 6th International Conference on Energy and Environmental Protection (2017) 1251-1254 (https://doi.org/10.2991/iceep-17.2017.219)
27. Y. Guo, Y. X. Zhang, K. Soe, R. Wuhrer, W. D. Hutchison, H. Timmers, *J. Cleaner Prod.* **313** (2021) 127682 (https://doi.org/10.1016/j.jclepro.2021.127682)
28. A. Pivák, M. Pavlíková, M. Záleská, M. Lojka, O. Jankovský, Z. Pavlík, *Materials* **13** (2020) 2537 (https://doi.org/10.3390/ma13112537)
29. M. S. Elfeky, A. Mohsen, A. Maher, M. Kohail, *Const. Build, Mat.* **342** (2022) 127976 (https://doi.org/10.1016/j.conbuildmat.2022.127976)
30. Q. Huang, W. Zheng, X. Xiao, J. Dong, J. Wen, C. Chang, *Ceramics Int.* **47** (2021) 34341-34351 (https://doi.org/10.1016/j.ceramint.2021.08.347)
31. IS 11803 – 1986: Magnesium oxide for explosive ammunition protective compositions and pyrotechnic industry (1986)
32. IS 254 – 1973: Specification for magnesium chloride (1973)
33. IS 10132 - 1982: Method of test for materials for use in the preparation of magnesium oxychloride flooring compositions (1982)
34. R. E. Dinnebier, I. Halasz, D. Freyer, J. C. Hanson, *Z. Anorg. Allg. Chem.* **637** (2011) 1458 (https://doi.org/10.1002/zaac.201100139)
35. T. Zhang, Q. Guo, X. Chen, C. Cheeseman, H. Wang, J. Chang, *Cement Conc. Compos.* **157** (2025) 105941 (https://doi.org/10.1016/j.cemconcomp.2025.105941)
36. E. A. Paukshtis, M. A. Yaranova, I. S. Batueva, B. S. Bal'zhinimaev, *Micropor. Mesopor. Mat.* **288** (2019) 109582 (https://doi.org/10.1016/j.micromeso.2019.109582)
37. Y. Hao, Y. Li, *Constr. Build. Mater.* **282** (2021) 122708 (https://doi.org/10.1016/j.conbuildmat.2021.122708).